Jan Chleboun; Lenka Dohnalová; Judita Rumcziková

On models of long-term behavior of concrete

In: Jan Chleboun and Pavel Kůs and Petr Přikryl and Miroslav Rozložník and Karel Segeth and Jakub Šístek (eds.): Programs and Algorithms of Numerical Mathematics, Proceedings of Seminar. Hejnice, June 21-26, 2020. Institute of Mathematics CAS, Prague, 2021. pp. 21–29.

Persistent URL: http://dml.cz/dmlcz/703097

Programs and Algorithms of Numerical Mathematics 20
J. Chleboun, P. Kůs, P. Přikryl, M. Rozložník, K. Segeth, J. Šístek (Eds.)
Institute of Mathematics of the Czech Academy of Sciences, Prague 2021

ON MODELS OF LONG-TERM BEHAVIOR OF CONCRETE

Jan Chleboun, Lenka Dohnalová, Judita Runcziková

Faculty of Civil Engineering, Czech Technical University in Prague
Thákurova 7, 166 29 Prague 6, Czech Republic
jan.chleboun@cvut.cz, lenka.dohnalova@fsv.cvut.cz, judita.runczikova@fsv.cvut.cz

Abstract: Long-term behavior of concrete is modeled by several widely accepted models, such as B3, *fib* MC 2010, or ACI 209 whose input parameters and output values are not identical to each other. Moreover, the input and, consequently, the output values are uncertain. In this paper, fuzzy input parameters are considered in uncertainty quantification of each model response and, finally, the sets of responses are analyzed by elementary tools of evidence theory. That is, belief and plausibility functions are proposed to combine evidence from different models.

Keywords: fuzzy sets, evidence theory, drying shrinkage, drying creep

MSC: 26E50, 74S99, 74-10

1. Introduction

The lifespan of a structure made of concrete is expected to be one hundred years. As a consequence, the question arises what the long-term prediction of its condition might be.

The time evolution of concrete material parameters and its other properties has been the subject of research for decades. The outcomes of the efforts of experimenters, analysts, and other specialists have materialized in various mathematical models of the long-term behavior of concrete. Some are widely accepted and used in civil engineering for the assessment of the long-term behavior of concrete structures. At least the B3 model [4], *fib* Model Code 2010 [7], ACI 209.2R-08 code [3], and Eurocode 2 [6] should be mentioned.

Among quantities that are in the focus of concrete-oriented civil engineers, only two are the subject of this paper, namely the drying shrinkage $\varepsilon_{\mathrm{sh}}$ and the drying creep compliance J_{d}. Since the readership is expected to be more mathematics- than engineering-oriented, let us limit ourselves to a brief characterization formulated in [5]: "Concrete drying is accompanied by its gradual contractive volume changes referred to as shrinkage and additional compliance called drying creep or the Pickett

DOI: 10.21136/panm.2020.02

effect. The complex interplay between shrinkage and creep determines the evolution of stresses and so its thorough analysis can help to identify potential cracking and thus to estimate the lifetime of a concrete structure."

The importance of the correct assessment of the impact that these phenomena can have on real structures has been demonstrated by, for instance, the disastrous fate of the Koror-Babeldaob Bridge (the Republic of Palau) [1] or the Morandi Bridge (Genoa, Italy) [2]. Both were prestressed concrete structures and both contended with problems caused by creep. The former collapsed in 1996, the latter in 2018.

The proposed models of the drying shrinkage and the drying creep compliance take the form of functions of the time variable, where, however, a number of other quantities are present as input parameters, see Section 3. These parameters must be considered uncertain (as explicitly stated in [4], for instance), though the models themselves are presented as crisp functions. From the viewpoint of uncertainty quantification, the functions are functions of several variables (see (3)–(7)), that is, of the time variable and the input quantities included in the uncertainty analysis.

The goal of this paper is to propose an approach that combines two sources of uncertainty: the use of different models of the same quantity, and the fuzziness of the input parameters of the models.

It must be emphasized that the focus is on presenting the approach, not on the particular definition of the fuzzified models. Their fuzzy parameters have been chosen to illustrate the idea and demonstrate the calculation of fuzzy outputs, not to assess a particular concrete structure.

2. Introduction to fuzzy sets

Although the most common approach is to represent uncertain input parameters by random variables or processes, a fuzzy set approach is used in this paper. The authors believe that it enables a more realistic assessment of the uncertainty in input parameters than a probabilistic approach that suffers from the lack of relevant probabilistic data.

A fuzzy number r is represented by a continuous membership function μ_r defined on $\mathbb{R}$ (the set of real numbers). The function μ_r is, for simplicity, concave or quasiconcave and with the range equal to the interval $[0, 1]$. The value $\mu_r(x)$ is called the grade of membership of x in the fuzzy set $A_r = (\mathbb{R}, \mu_r)$. The fuzzy set A_r is equivalently characterized by the set of intervals $I^\alpha_{A_r} = \{x \in \mathbb{R} |\ \mu_r(x) \geq \alpha\}$, where $\alpha \in (0, 1]$ and $I^0_{A_r}$ is the closure of $\cup_{\alpha\in(0,1]} I^\alpha_{A_r}$. The intervals $I^\alpha_{A_r}$ are called the α-cuts or α-level sets of A_r. If a set of embedded intervals I^α_A, where $\alpha \in (0, 1]$, is given, then the associated membership function μ_A is defined by $\mu_A(x) = \sup\{\alpha |\ x \in I^\alpha_A\}$.

If a function of one real variable is given and its variable takes values from a fuzzy set, the range of the function forms an output fuzzy set. The goal is to characterize its fuzziness.

Let us assume that a continuous function f is defined on the interval I^0_A and that the associated membership function μ_A is given, too. Let $f(A)$ denote the

range of f, then $\mu_{f(A)}$, the membership function of $f(A)$, is obtained by the Zadeh extension principle [8, Section 2.1.7]

$$\mu_{f(A)}(y) = \sup\{\mu_A(x)|\ f(x) = y\}. \tag{1}$$

Under the continuity and convexity assumptions made on μ_A, the membership function $\mu_{f(A)}$ can be reconstructed from the family of the α-cuts of $f(A)$, see [8, Section 2.1.7], that are defined as follows:

$$I^{\alpha}_{f(A)} = \left[\min_{x \in I^{\alpha}_A} f(x),\ \max_{x \in I^{\alpha}_A} f(x)\right]; \tag{2}$$

the minimum and maximum are attained owing to the continuity of f and the compactness of I^{α}_A.

If f is a function of n variables such that their values x_i belong to fuzzy sets A_i associated with membership functions μ_i, an i-dependent system of $I^{\alpha}_{A_i}$, the α-cuts of each A_i, is defined. Moreover, α-cuts of $A = A_1 \times \cdots \times A_n$ can easily be defined as $I^{\alpha}_A = \{x \in A|\ \mu_i(x_i) \geq \alpha,\ i = 1, \ldots, n\}$. Then the Zadeh extension principle can again be applied in its original form (1) or in the computationally more convenient form (2), where global extremes are searched for on rectangular parallelepipeds I^{α}_A.

3. Crisp models of long-term behavior of concrete

Three models of the drying shrinkage $\varepsilon_{\mathrm{sh}}$ and the drying creep compliance J_{d} were taken into consideration, namely the B3 model [4], *fib* Model Code 2010 [7], and ACI 209.2R-08 code [3].

The models are rather phenomenological and depend on a number of material, physical, or technological parameters. Not all of the parameters are shared by all the models. Since a full description of the relationships included in the $\varepsilon_{\mathrm{sh}}$ and J_{d} functions is out of the scope of this contribution, let us concentrate on only those parameters that will be considered uncertain, and let us substitute the respective numerical values for the other parameters, that is, fixed parameters. These include, for instance, the modulus of elasticity at the age of 28 days (28 178 MPa), cement content (409 kg/m^3), start of drying (7 days), start of loading (7 days), the type of cement and its particular sort, the aggregate type, etc.

To give the reader an impression of the functions $\varepsilon_{\mathrm{sh}}$ and J_{d}, let us show the expressions in the *fib* Model Code 2010 after substituting numerical values for the fixed parameters and after rounding to a few significant digits

$$J_{\mathrm{d}}^{fib\mathrm{MC}}(t) = 0.12 \frac{f_{\mathrm{cm}}^{-1.7}(1 - h_{\mathrm{RH}})}{\sqrt[3]{D}} \left(\frac{t-7}{m+t-7}\right)^{0.28}, \tag{3}$$

where

$$m = \min\left\{8874\,\sqrt{f_{\mathrm{cm}}^{-1}}, 1.5\,D + 1479\,\sqrt{f_{\mathrm{cm}}^{-1}}\right\}; \tag{4}$$

$$\varepsilon_{\mathrm{sh}}^{fib\mathrm{MC}}(t) = 0.001023\,\mathrm{e}^{-0.012\,f_{\mathrm{cm}}}\left(1 - h_{\mathrm{RH}}^3\right)\left(\frac{t-7}{0.035\,D^2 + t - 7}\right)^{0.5}. \tag{5}$$

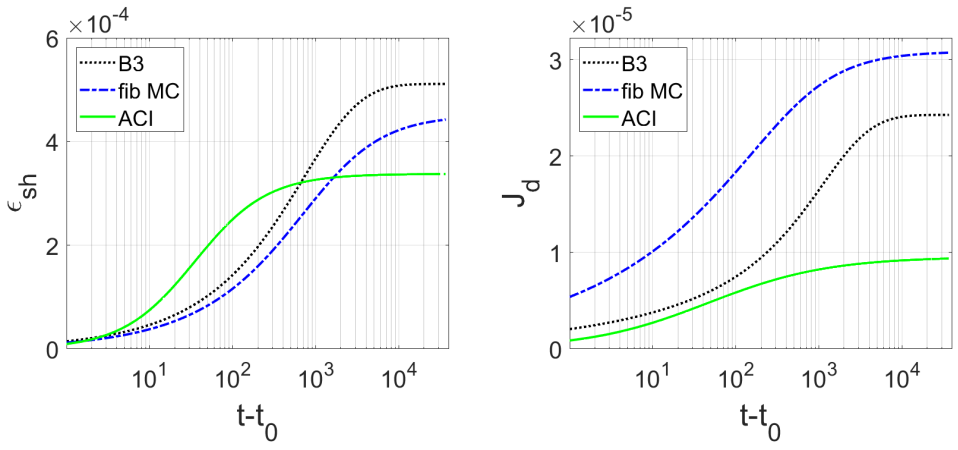

Figure 1: Drying shrinkage $\varepsilon_{\mathrm{sh}}$ and drying creep compliance J_{d} graphs; t_0 is equal to seven (days).

Only four non-numerical symbols appear in (3)-(5), these represent the average relative humidity of the environment (h_{RH}), the mean compression strength (f_{cm}), and a parameter related to the volume-surface ratio of the modeled structural element (D). The time (in days) is denoted by t and considered in the interval $I_{\mathrm{T}} = (7, 36500]$.

The other models are also represented by nonlinear functions. For the B3 model, for instance, we obtain

$$J_{\mathrm{d}}^{\mathrm{B3}}(t) = \frac{0.723\sqrt{\mathrm{e}^{-8+8(1-h_{\mathrm{RH}})\tanh(\phi(t))} - 0.0003354}}{f_{\mathrm{cm}}\left(0.019\, w^{2.1} f_{\mathrm{cm}}^{-0.28} + 270\right)^{0.6} \gamma^{0.6}}, \tag{6}$$

$$\varepsilon_{\mathrm{sh}}^{\mathrm{B3}}(t) = 1.08 \cdot 10^{-6} \left(0.019\, w^{2.1} {f_{\mathrm{cm}}}^{-0.28} + 270\right) \gamma \left(1 - {h_{\mathrm{RH}}}^3\right) \tanh\left(\phi(t)\right), \tag{7}$$

where w, which is not used in the *fib* MC model, stands for the water content of a concrete mixture, and

$$\phi(t) = 3.71\sqrt{\frac{(t-7)\sqrt[4]{f_{\mathrm{cm}}}}{D^2}}, \qquad \gamma = \sqrt{\frac{11.63\sqrt[4]{f_{\mathrm{cm}}} + 0.072\, D^2}{8.18\sqrt[4]{f_{\mathrm{cm}}} + 0.085\, D^2}}.$$

To give the reader an idea of J_d (in 1/MPa) and $\varepsilon_{\mathrm{sh}}$ graphs, typical curves are depicted in Figure 1. The values $w = 205\ \mathrm{kg\,m^{-3}}$, $h_{\mathrm{RH}} = 0.7$, $f_{\mathrm{cm}} = 33.3$ MPa, and $D = 200$ mm are used in (3), (5), (6), and (7) as well as in the other model. The shapes of the J_d and $\varepsilon_{\mathrm{sh}}$ graphs are similar, though the models are not fully comparable because the sets of their input parameters are not identical. A brief summary and comparison of the models is available in [5].

4. Fuzzification of the models

The common approach to the fuzzification of the B3, *fib* MC 2010, and ACI models is used. That is, some input parameters are represented by fuzzy numbers.

These are the already mentioned f_{cm}, h_{RH}, and D. One additional fuzzy parameter (water content w) is used in the B3 model and four additional fuzzy parameters are considered in the *fib* MC 2010 model (slump of concrete slurry, ratio of fine to total aggregate, air content, and cement content). The other parameters (not listed here) remain crisp and fixed.

The trapezoidal form of fuzzy numbers is applied. To give a few examples, let us list $[0.92, 0.99, 1.01, 1.08]\widehat{w}$, $[0.9, 0.97, 1.03, 1.1]\widehat{f}_{\mathrm{cm}}$, $[0.92, 0.99, 1.01, 1.08]\widehat{h}_{\mathrm{RH}}$, or $[0.93, 0.99, 1.01, 1.07]\widehat{D}$, where $[a, b, c, d]\widehat{q}$ stands for the fuzzy set determined by the α-cuts (i.e., intervals) $[(1-\alpha)a + \alpha b,\ \alpha c + (1-\alpha)d]$ multiplied by the representative crisp value of an input quantity $\widehat{q}$.

Let us indicate the dependence of the drying shrinkage and the drying creep compliance on the model. That is, the functions $\varepsilon^*_{\mathrm{sh}}$, and J^*_{d} are introduced, where $*$ is replaced by B3, *fib*MC, and ACI. From the mathematical point of view, the input variables of these functions are fuzzy numbers except for time t; for computational purposes, the fuzzy inputs are represented by real variables in the α-level intervals.

It is convenient to define A_{B3}, $A_{\mathit{fib}\mathrm{MC}}$, and A_{ACI}, the fuzzy sets of inputs, through their α-cuts that are, in fact, products of the α-cuts of the relevant variables. For example, $A^{\alpha}_{\mathrm{ACI}} = I^{\alpha}_{f_{\mathrm{cm}},\mathrm{ACI}} \times I^{\alpha}_{h_{\mathrm{RH}},\mathrm{ACI}} \times I^{\alpha}_{D,\mathrm{ACI}}$. Although the models share some uncertain input parameters, their respective fuzzy sets of inputs can be different in practice.

By switching from single input values to intervals of input values, we obtain α-dependent sets of $\varepsilon_{\mathrm{sh}}$ and J_d curves over the interval I_{T}. Although these represent fuzzy sets, they are not suitable for further uncertainty analysis. Instead of monitoring the entire evolution, it is more convenient to record $\varepsilon_{\mathrm{sh}}$ and J_d at fixed time points $t_1, t_2, \ldots, t_n \in I_{\mathrm{T}}$.

To obtain the model-dependent fuzzy sets of the output drying shrinkage and drying creep compliance at each discrete time point $t_1, t_2, \ldots, t_n$, the α-cut–based technique (2) is applied, where f is replaced by $\varepsilon_{\mathrm{sh}}$ and J_d with the superscript indicating the model.

In (2), the global extrema must be found. To this end, sensitivity analysis is performed by the differentiation of the drying shrinkage and drying creep compliance with respect to the uncertain parameters. By using a computer algebra system, one can show monotonicity properties of the functions, which makes the search for the extrema quite simple as these are attained at corner points whose position is easily identifiable on the basis of the sign of the partial derivatives of $\varepsilon_{\mathrm{sh}}$ and J_d. The analyst, however, should be aware of a minor complication due to the non-differentiability at some (usually h_{RH}) points because a few dependencies are expressed in a piecewise manner in the models, see (4).

5. Evaluation of the outputs of the models

Instead of the interval $[0, 1]$, a finite set $S = \{\alpha_0, \alpha_1, \ldots, \alpha_L\} \subset [0, 1]$ is considered to determine the α-cuts, where $\alpha_0 = 0 < \alpha_1 < \cdots < \alpha_L = 1$.

For each $\alpha_i \in S$, intervals $I^{\alpha_i}_{\varepsilon^{B3}_{\rm sh}}$, $I^{\alpha_i}_{\varepsilon^{ACI}_{\rm sh}}$, and $I^{\alpha_i}_{\varepsilon^{fibMC}_{\rm sh}}$ result from solving (2) with the drying shrinkage function on the α_i-cuts of $A_{\rm B3}$, $A_{\rm ACI}$, and $A_{fib\rm MC}$, respectively. The intervals $I^{\alpha_i}_{J^{\rm B3}_d}$, $I^{\alpha_i}_{J^{\rm ACI}_d}$, and $I^{\alpha_i}_{J^{fib\rm MC}_d}$ are obtained in a similar manner for the drying creep compliance.

An illustrative example of such outputs is presented in Figure 2 for $\alpha = 0.25$ and $t = 3650$. The B3, *fib*, and ACI output intervals are indicated by the dotted, dashed, and solid line segments, respectively. Though the intervals overlap, the line segments are vertically separated to be easily visually comparable.

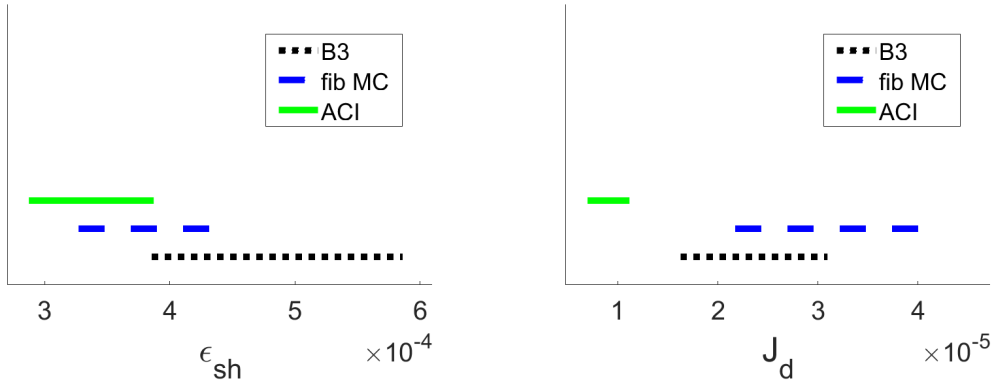

Figure 2: Left: The intervals $I^{0.25}_{\varepsilon^{\rm B3}_{\rm sh}}$, $I^{0.25}_{\varepsilon^{fib\rm MC}_{\rm sh}}$, and $I^{0.25}_{\varepsilon^{\rm ACI}_{\rm sh}}$. Right: The intervals $I^{0.25}_{J^{\rm B3}_d}$, $I^{0.25}_{J^{fib\rm MC}_d}$, and $I^{0.25}_{J^{\rm ACI}_d}$.

We observe that, in this setting of input data, the response of the three models is more consistent for the drying shrinkage $\varepsilon_{\rm sh}$ than for the drying creep compliance J_d. It holds $I^{0.25}_{\varepsilon^{\rm B3}_{\rm sh}} \cap I^{0.25}_{\varepsilon^{\rm ACI}_{\rm sh}} \cap I^{0.25}_{\varepsilon^{fib\rm MC}_{\rm sh}} = [3.85, 3.87] \times 10^{-4}$.

5.1. Application of evidence theory

Instead of a simple union and intersection of the output intervals, another and more sophisticated approach can be used to assess the combined response of the models.

Evidence (also known as Dempster–Shafer) theory allows for the combination of evidence from different sources, see, for instance, [9, 10]. In this approach, a (finite, for simplicity) subset $\mathcal{F}$ of $P(X)$, the power set of the universal set X, is fixed and its elements are evaluated through a mapping $m : \mathcal{F} \to [0, 1]$ (called the basic probability assignment) in such a way that

$$m(\emptyset) = 0, \quad \text{and} \quad \sum_{A \in \mathcal{F}} m(A) = 1.$$

Then, two measures are defined on $P(X)$, namely *Belief* (*Bel*) and *Plausibility* (*Pl*):

$$Bel(A) = \sum_{\{B\in\mathcal{F}:\ B\subseteq A\}} m(B) \quad \text{and} \quad Pl(A) = \sum_{\{B\in\mathcal{F}:\ B\cap A\neq\emptyset\}} m(B), \tag{8}$$

where $A \in P(X)$.

Belief and *Plausibility* are often interpreted as lower and upper bounds on probabilities [9, 10], but, for our purposes, we can interpret them simply as lower and upper bounds on the combination of weighted outputs of the models.

To this end, let for each $\alpha_i \in S$, the three intervals $I^{\alpha_i}_{\varepsilon^{B3}_{\text{sh}}}$, $I^{\alpha_i}_{\varepsilon^{ACI}_{\text{sh}}}$, and $I^{\alpha_i}_{\varepsilon^{fibMC}_{\text{sh}}}$ form the set $\mathcal{F}_{\alpha_i}$ and $m(I^{\alpha_i}_{\varepsilon^{B3}_{\text{sh}}}) = w_{\text{B3}}$, $m(I^{\alpha_i}_{\varepsilon^{ACI}_{\text{sh}}}) = w_{\text{ACI}}$, and $m(I^{\alpha_i}_{\varepsilon^{fibMC}_{\text{sh}}}) = w_{fib\text{MC}}$, where w_{B3}, w_{ACI}, and $w_{fib\text{MC}}$ are fixed, α_i-independent positive weights whose sum is equal to one.

Then, $Bel^{\alpha_i}_{\varepsilon_{\text{sh}}}(I)$ and $Pl^{\alpha_i}_{\varepsilon_{\text{sh}}}(I)$ can be calculated for any interval $I \subset \mathbb{R}$ and $\alpha_i \in S$. In parallel, the same steps can be applied to the intervals $I^{\alpha_i}_{J_d^{\text{B3}}}$, $I^{\alpha_i}_{J_d^{\text{ACI}}}$, and $I^{\alpha_i}_{J_d^{fib\text{MC}}}$ to obtain $Bel^{\alpha_i}_{J_d}(I)$ and $Pl^{\alpha_i}_{J_d}(I)$.

Examples: Let $w_{\text{B3}} = 0.4$, $w_{\text{ACI}} = 0.25$, $w_{fib\text{MC}} = 0.35$, and $I_1 = [3.2, 4.4]\times 10^{-4}$, then the interval I_1 fully covers the ε_{sh} output of the *fib* MC model and intersects the ε_{sh} output intervals of the B3 and ACI models, see Figure 3 (left). As a consequence of (8), $Bel^{0.25}_{\varepsilon_{\text{sh}}}(I_1) = w_{fib\text{MC}} = 0.35$ and $Pl^{0.25}_{\varepsilon_{\text{sh}}}(I_1) = w_{\text{B3}} + w_{\text{ACI}} + w_{fib\text{MC}} = 1$. We can conclude that given the 0.25-level of uncertainty in the considered input data and the ten-year time, the range of the drying shrinkage ε_{sh} represented by the interval I_1 contains the entire response of the *fib* MC model and intersect the responses of the B3 and ACI models. That is, I_1 is, to some degree, consistent with the B3 and ACI responses. However, the degree of consistency (i.e., the size of the intersection) is not assessed in Dempster-Shafer theory.

The interval $I_2 = [2.8, 4.4] \times 10^{-4}$ fully covers the ε_{sh} output of the *fib* MC and ACI models and intersects the ε_{sh} output interval of the B3 model, see Figure 3 (left). We obtain $Bel^{0.25}_{\varepsilon_{\text{sh}}}(I_2) = w_{fib\text{MC}} + w_{\text{ACI}} = 0.35 + 0.25 = 0.6$ and $Pl^{0.25}_{\varepsilon_{\text{sh}}}(I_2) = 1$.

If $I_3 = [1, 2.3] \times 10^{-5}$, for example, then $Bel^{0.25}_{J_d}(I_3) = 0$ and $Pl^{0.25}_{J_d}(I_3) = 1$ as can be seen in Figure 3 (right).

Let us emphasize that the *Bel* and *Pl* function values can be calculated for any interval. One can, for example, search for the shortest interval K_1 such that $Pl(K_1) > Bel(K_1) > 0$. Then K_1 encompasses the output of at least one model and is consistent with the output of at least one other model. As a consequence, the analyst can consider K_1 as the range of an output quantity that is fully related to at least one model and partially supported by at least one other model. The intensity of the relationship between the interval K_1 and the output intervals delivered by the models is represented by the *Bel* and *Pl* values that are also related to the credibility of the models (see w_{B3}, w_{ACI}, and $w_{fib\text{MC}}$). More constraints can be incorporated into the search. Take $1 = Pl(K_2) > Bel(K_2) > 0$ or $1 = Pl(K_3) > Bel(K_3) \geq 0.4$, for instance.

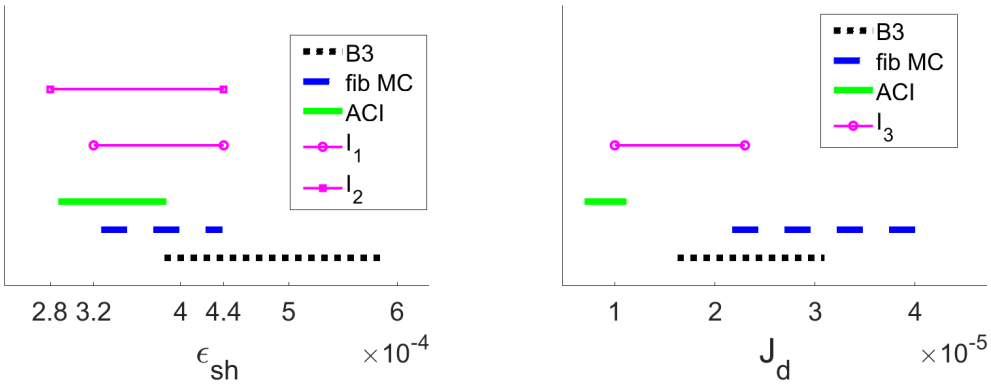

Figure 3: Left: $Bel^{0.25}_{\varepsilon_{\rm sh}}(I_1) = 0.35$, $Pl^{0.25}_{\varepsilon_{\rm sh}}(I_1) = 1$, $Bel^{0.25}_{\varepsilon_{\rm sh}}(I_2) = 0.6$, $Pl^{0.25}_{\varepsilon_{\rm sh}}(I_2) = 1$. Right: $Bel^{0.25}_{J_d}(I_3) = 0$, $Pl^{0.25}_{J_d}(I_3) = 1$

.

6. Conclusions

The fuzzy set approach is standard and results in a number of model responses associated with various models, α levels, and times. The fact that different models of the long-term behavior of concrete are available is utilized for the combination of their responses. Dempster–Shafer (evidence) theory offers tools for testing the degree of compatibility of proposed intervals with the model responses that originate from uncertainty in input data. The *Belief* and *Plausibility* values help the analyst to identify a weighted extent of uncertainty in the combined outputs of several models. Although the subjective role of the analyst is still present through the definition of input membership functions and the weights of the models, the rest of the analysis is algorithmic. Moreover, Dempster–Shafer theory allows the combination of results obtained under different weights of the models [9, 10], which permits to take into account different expert opinions on the weights of the models.

Acknowledgements

This work of the first and third author was supported by the Grant Agency of the Czech Technical University in Prague, grant No. SGS20/004/OHK1/1T/11. The work of the second author was supported by the Czech Science Foundation, grant No. 19-20666S.

References

[1] https://en.wikipedia.org/wiki/Koror-Babeldaob_Bridge. Accessed on September 20, 2020.

[2] https://en.wikipedia.org/wiki/Ponte_Morandi. Accessed on September 20, 2020.

[3] ACI Committee 209: *Guide for Modeling and Calculating Shrinkage and Creep in Hardened Concrete (ACI 209.2R-08)*. American Concrete Institute, Farmington Hills, Michigan, USA. Available at http://www.civil.northwestern.edu/people/bazant/PDFs/Papers/R21.pdf, accessed on September 27, 2020.

[4] Bažant, Z. P. and Baweja, S.: Creep and Shrinkage Prediction Model for Analysis and Design of Concrete Structures: Model B3. In: A. Al-Manaseer (Ed.), *The Adam Neville Symposium: Creep and Shrinkage-Structural Design Effects*, *ACI SP*, vol. 194, pp. 1–83. American Concrete Institute, Farmington Hills, Michigan, USA, 2000. Available at http://www.civil.northwestern.edu/people/bazant/PDFs/Papers/S39.pdf, accessed on September 27, 2020.

[5] Dohnalová, L. and Havlásek, P.: Comparison of drying shrinkage and drying creep kinetics in concrete. In: P. Padevět (Ed.), *9th annual Conference NANO & MACRO MECHANICS 2018*, *Acta Polytecnica CTU Proceedings*, vol. 15, pp. 12–19. Czech Tecnical University in Prague, Prague, 2018. Available at https://ojs.cvut.cz/ojs/index.php/APP/article/view/5314/4886, accessed on September 2, 2020.

[6] European Commision: EN 1992: Design of concrete structures, 1992. Czech adoption: Český normalizační institut: Eurokód 2: Navrhování betonových konstrukcí – Část 1-1: Obecná pravidla a pravidla pro pozemní stavby. Český normalizační institut, Praha, 1996.

[7] Fédération internationale du béton: *fib Model Code for Concrete Structures 2010*. Ernst & Sohn, Berlin, 2013.

[8] Möller, B. and Beer, M.: *Fuzzy Randomness: Uncertainty in Civil Engineering and Computational Mechanics*. Springer-Verlag, Berlin, 2004.

[9] Sentz, K. and Ferson, S.: Combination of evidence in dempster–shafer theory. Tech. Rep. SAND2002-0835, Sandia National Laboratories, Albuquerque, New Mexico 87185 and Livermore, California 94550, 2002. Available at https://core.ac.uk/download/pdf/205693693.pdf, accessed on September 4, 2020.

[10] Shafer, G.: *A Mathematical Theory of Evidence*. Princeton University Press, Princeton, 1976.